Supporting Information

Henry and Obleser 10.1073/pnas.1213390109

SI Results

Electrophysiological Correlates of Gap Detection. After demonstrating the dependence of gap detection on delta brain phase, we examined the electrophysiological correlates of detected versus undetected gaps. Fig. S4*A* shows event-related potentials (ERPs) elicited by detected and undetected gaps, averaged over all electrodes, with regions of significant difference marked in red [based on the Fieldtrip-implemented, false discovery rate (FDR)-corrected, paired-samples permutation *t* test, with cluster correction; ref. 1]. It is clear that ERPs to detected gaps were overall larger than ERPs to undetected gaps.

Results for power changes (Fig. S4*B*) and intertrial phase coherence (ITPC) (Fig. S4*C*) in response to gaps revealed converging results. That is, both metrics revealed significant differences spanning the delta, theta, and alpha bands (2–12 Hz) in the time window corresponding to the gap-evoked response. With respect to power, a significant enhancement was observed in a single cluster spanning the delta and theta bands (2–8 Hz). Suppression was observed in the alpha (two clusters, one impinging on theta: 9–11 Hz, 6–10 Hz) and beta (one cluster: 15–25 Hz) bands, that was stronger for detected than for undetected gaps. Similarly, ITPC in the delta, theta, and alpha bands (single significant cluster: 2–15 Hz frequency range) was increased for detected relative to undetected gaps, also in the time range of the ERP. Thus, both power and phase coherence results suggest enhancement of the phase-locked evoked response to detected relative to undetected gaps.

We also calculated a bifurcation index (2), which indexes the consistency of the phase reset due to detected versus undetected gaps (Fig. S4*D*). Negative values indicate stronger phase concentration for one target type (e.g., hits) than for the other (e.g., misses), whereas positive values indicate phase consistency for both hits and misses, but with different preferred phase angles. The value of the bifurcation index was significantly negative relative to the pretarget baseline period (–1 to –0.5 s) in the delta, theta, and alpha frequency bands (2–12 Hz) for 600 ms after target occurrence. Taken together with the ITPC results, gap-evoked responses were consistent following detected targets, whereas undetected targets did not reset phase in the 2- to 12-Hz range to a consistent angle.

Delta Phase is a Better Predictor of ERP Magnitude than Target Detection. We also compared the degree to which ERP magnitudes correlated with hit rates versus delta phase. As would be expected, N1 [$t_{(11)} = 5.21$, $P > 0.001$] and P2 [$t_{(11)} = 1.98$, $P = 0.07$] amplitudes were significantly correlated with hit rate (this was only marginal for P2 amplitude). We wanted to rule out the possibility that the relation between the neural delta oscillation and ERP was merely a by-product of more detected targets (with therefore larger ERPs) occurring near the peak of the delta oscillation. If modulation of ERPs by delta phase was simply due to more hits occurring in some delta phases than in others, we would have expected the hit rate–ERP correlation to be greater than or equal to the delta phase–ERP correlation. However, delta phase [N1: $t_{(11)} = 8.35$, P2: $t_{(11)} = 10.08$] predicted ERP amplitudes better than hit rate ($P < 0.001$), indicating that phase effects were not simply the result of more detected targets for some delta phases relative to others.

Conditional Probability of Gap Detection. We also conducted an analysis in which we calculated hit rates as a function of the time since the previous target occurrence. Each stimulus contained between two and four gaps, and the minimum duration between gaps was 667 ms. Thus, gaps occasionally occurred in the time window of the phase-reset response evoked by the previous gap (the "ERP window"). Because hits and misses had significantly different gap-evoked response signatures, it was possible that estimating instantaneous phase in this time window may have been in part responsible for the delta phase effects we observed.

Thus, we examined detection performance for only those gaps that followed another target within the same 10-s stimulus. We binned these gaps based on the duration separating them from the preceding target (1–6 s; we ignored gaps occurring after a longer duration because there were too few of these trials to provide a meaningful comparison). Moreover, we split the gaps according to whether the preceding target was a hit (and thus elicited a phase reset) or a miss (and was less likely to elicit a phase reset). Fig. S5 shows hit rates as a function of time since the preceding gap, split according to whether the previous target was a hit or a miss. A repeated-measures ANOVA revealed a significant main effect of time since the previous gap ($P = 0.001$), which was qualified by a significant interaction with whether the previous gap was a hit or miss ($P = 0.02$). The interaction was driven by lower hit rates for gaps occurring within 1 s of a detected gap than an undetected gap ($P = 0.005$); pairwise comparisons of hit rates for gaps following hits vs. misses did not reach significance at any other time point ($P > 0.2$).

This analysis indicated that gaps occurring within the ERP time window of another detected gap were more likely to be missed than if the preceding gap was not detected and, thus, did not produce a strong phase reset. To rule out that the observed delta phase effects were an artifact of this result, we removed all trials on which the gap occurred within 1 s of another gap, regardless of whether the preceding gap was a hit or miss. Then, we replicated our analysis that involved sorting trials by delta phase (Fig. 4). Critically, we found that even without trials where gaps occurred within an ERP window, delta phase significantly predicted hit rate ($t = 18.98$, $P < 0.001$, rms $\rho = 0.87$), N1 amplitude ($t = 183.22$, $P < 0.001$, rms $\rho = 0.99$), and P2 amplitude ($t = 28.16$, $P < 0.001$, $\rho = 0.98$). We thus conclude that our delta phase results were not simply due to occasionally presenting a target in the time window of the phase-reset response evoked by the previous gap.

SI Experimental Procedures

Procedure. Titration of individual gap duration was accomplished by using a two-down one-up adaptive tracking procedure, which converged on the gap duration corresponding to 70.7% correct in a three-alternative forced-choice (3AFC) gap detection task (3, 4) in MATLAB on a MacBook Pro laptop (Apple). On each trial, listeners were presented with three 1-s FM stimuli, constructed according to the same constraints as the stimuli in the experiment proper, and indicated which of the three contained a gap. The gap was always temporally centered in the stimulus. The starting phase of each of the three stimuli was randomized independently and could take on any value between 0 and 2π, Thus, gaps occurred during the thresholding procedure equally often at all stimulus phases. Thresholds were therefore an approximate average of individual thresholds corresponding to different stimulus phase locations. Listeners completed three blocks of the adaptive tracking procedure in ~15 min. Twelve reversals were completed during each block, and thresholds were taken as the arithmetic average of the final eight reversals. The final individual gap duration was taken as the average of the three estimates from the individual blocks.

For the main experiment, listeners were seated in front of a black-screen computer monitor in an EEG cabin. They registered responses with a button box, which they were permitted to hold in their

lap or set on the table in front of them. Each trial was initiated with a button press, which was followed by the appearance of a fixation cross after a variable interval (centered on 1.5 s), and after another variable interval (centered on 1.5 s) by the onset of the sound. The experiment was self paced, in that listeners were allowed to break as long as they wished before initiating the next trial.

Data Analysis. ***Behavioral data.*** Behavioral performance was modulated by the FM phase at which the to-be-detected gap occurred. To confirm this observation, separate circular–linear correlations were calculated between stimulus phase and hit rate for each listener. To test the strength of these correlations across listeners, correlations were first converted to coefficients of determination (R^2) by squaring, and then arcsine transformed to overcome nonnormality due to bounding of circular-linear correlations between 0 and 1 (5). Squared, transformed correlation coefficients were then tested against the null hypothesis of zero correlation.

EEG data. Two sets of epochs-of-interest were defined. Full-stimulus epochs were defined as 1.5 s preceding and 11.5 s after the sound onset to capture the full 10-s stimulus. Target epochs were defined as 2 s preceding and 2 s after each gap occurrence. Data were bandpass filtered between 0.1 Hz and 100 Hz, then artifacts were rejected in two steps. First, independent components analysis (ICA) was used to eliminate blinks, electrooculuogram (EOG), and muscle activity. For full-stimulus epochs, this procedure resulted in removal of $M = 4.27 \pm 1.37$ components (range: 2–7), and for target epochs, $M = 4.92 \pm 1.44$ components were removed (range: 3–7). Second, individual trials were automatically rejected by using a threshold-based rejection routine with a threshold of 120 μV. For full-stimulus epochs, after ICA, 5.2 ± 6.1% of trials were removed (range 1–38 of 210 trials), and for target epochs, 21 ± 11% of trials were removed (range 28–262 of 600 trials).

To examine oscillatory brain responses entrained by the 3-Hz stimulation, full-stimulus epochs were analyzed in the frequency domain. It should be noted that the starting phase of the FM stimulus was randomized from trial to trial. Therefore, before conducting frequency-domain analyses, brain responses were shifted in time so that the FM stimulus on each trial would have been perfectly phase-locked across trials. To estimate power in each frequency band, a fast Fourier transform (FFT) was performed on the trial-averaged time-domain data, after high-pass filtering at 0.5 Hz to reduce $1/f$ noise and multiplication with a Hann window. The single-trial time-domain data were submitted to a time–frequency analysis by using the Fieldtrip-implemented version of the Wavelet approach using Morlet wavelets (6, 7), with which the time series were convolved. Wavelet-based approaches to estimating time–frequency representations of EEG data form a good compromise between frequency and time resolution. Here, wavelet size varied with frequency linearly from three to seven cycles over the range from 1 to 15 Hz (Fig. 2 shows only up to 10 Hz). The resulting complex values were used to estimate ITPC (8) for each channel, for each frequency–time bin. ITPC was calculated according the formula

$$\mathrm{ITPC}_{(c,f,t)} = \frac{1}{N}\left|\sum_{k=1}^{N} e^{i\theta(c,f,t,k)}\right|,$$

where $\theta(c,f,t,k)$ is the single-trial, instantaneous phase angle of the ongoing oscillation on a single trial (k). The value of phase coherence is equal to the resultant vector length of the sample of phase angles and is bounded between a minimum of 0 and a maximum of 1. Because phase coherence values are bounded and are therefore not normally distributed, values were arcsine-transformed (5) before being submitted to statistical analysis.

Target epochs were first analyzed in the time domain; data for detected and undetected gaps were time locked with respect to gap onset, then low-pass filtered below 15 Hz and subjected to a paired-samples t test with a cluster-based correction for multiple comparisons (1). Target epochs were also subjected to a wavelet analysis; the complex output of the wavelet convolution was used to estimate power and ITPC separately for detected and undetected gaps, which were again compared with a paired-samples t test with cluster correction. Finally, ITPC values were used to estimate a bifurcation index (2), which can be calculated according to the formula:

$$(\mathrm{ITPC_d} - \mathrm{ITPC_T}) \times (\mathrm{ITPC_u} - \mathrm{ITPC_T}),$$

where $\mathrm{ITPC_d}$ refers to ITPC across all trials on which the target was detected, $\mathrm{ITPC_u}$ refers to ITPC across undetected target trials, and $\mathrm{ITPC_T}$ refers to the total ITPC over all trials. For the bifurcation index, negative values indicate significant phase concentration of either detected or undetected target trials (but not both), whereas positive values indicate significant phase concentration for both trial types, but with a different mean phase angle. Values near zero indicate that either both trial types are phase locked with the same mean angle or phase distributions for both trial types are uniform.

Trials were low-pass filtered with a 100-sample kernel. To estimate the relationship of ERP component amplitudes to neural delta phase at the time of target occurrence, mean amplitudes were extracted from time windows centered on the canonical N1 (50–150 ms) and P2 (150–250 ms) components. Random-effects analyses involved calculating circular-linear correlations between delta phase and each of these dependent measures for each listener. The correlation coefficients were first transformed to coefficients of determination by squaring, so that they would be additive and amenable to statistics. Then, because circular-linear correlation coefficients are bounded between 0 and 1, coefficients of determination were arcsine transformed before being submitted to single-sample t tests against 0. This analysis was repeated for stimulus phase (Fig. S3).

Optimal phase was estimated for each dependent variable [hit rate, response time (RT), ERP amplitude] with respect to both the stimulus and the brain by using the following procedure. Single-trial phase values were used to sort hits and ERPs for single trials into 20 bins corresponding to the same phase values as shown in Fig. 1. N1 and P2 time windows were defined the same as above. Thus, as for stimulus phase, the result was 20 hit rates, RTs, and ERPs, corresponding to 20 phase bins.

Binned data (for both stimulus and brain phase) were smoothed by using a circular smoothing method with a five-sample kernel. Then, for each listener, a single-cycle cosine function was fit to the smoothed data by using a MATLAB-implemented least squares routine (lsqcurvfit):

$$f(j) = \cos(2\pi f_{\mathrm{m}} t(j) + \varphi),$$

where $t(j)$ is the time step (t = 0–0.33 s), f_{m} was fixed at 3 Hz, and the phase lag parameter, φ, was free. Using the best-fit equation, we estimated the time step, $t(j)$, at which the function reached a local maximum (hits, P2) or minimum (RT, N1), corresponding to peak performance. The value of $t(j)$ yielding best performance was then multiplied by $2\pi f_{\mathrm{m}}$, where $f_{\mathrm{m}} = 3$, yielding the phase angle in radians corresponding to peak performance, i.e., optimal phase. Optimal phases were tested against uniformity by using Rayleigh tests.

Phase lag parameters for behavioral and electrophysiological data with respect to the stimulus and with respect to the brain were maintained and treated as estimates of the stimulus–behavior lag and brain–behavior lag, respectively. As outlined in

the main text, the combination of the brain–behavior lag and the stimulus–brain lag (estimated from cross-correlations between the stimulus and time-domain signal) was used to predict the brain–behavior lag.

1. Maris E, Oostenveld R (2007) Nonparametric statistical testing of EEG- and MEG-data. *J Neurosci Methods* 164(1):177–190.
2. Busch NA, Dubois J, VanRullen R (2009) The phase of ongoing EEG oscillations predicts visual perception. *J Neurosci* 29(24):7869–7876.
3. Leek MR (2001) Adaptive procedures in psychophysical research. *Percept Psychophys* 63(8):1279–1292.
4. Levitt H (1971) Transformed up-down methods in psychoacoustics. *J Acoust Soc Am* 49(2):2, 467.
5. Studebaker GA (1985) A "rationalized" arcsine transform. *J Speech Hear Res* 28(3): 455–462.
6. Tallon-Baudry C, Bertrand O (1999) Oscillatory gamma activity in humans and its role in object representation. *Trends Cogn Sci* 3(4):151–162.
7. Tallon-Baudry C, Bertrand O, Delpuech C, Permier J (1997) Oscillatory gamma-band (30-70 Hz) activity induced by a visual search task in humans. *J Neurosci* 17(2):722–734.
8. Lachaux J-P, Rodriguez E, Martinerie J, Varela FJ (1999) Measuring phase synchrony in brain signals. *Hum Brain Mapp* 8(4):194–208.

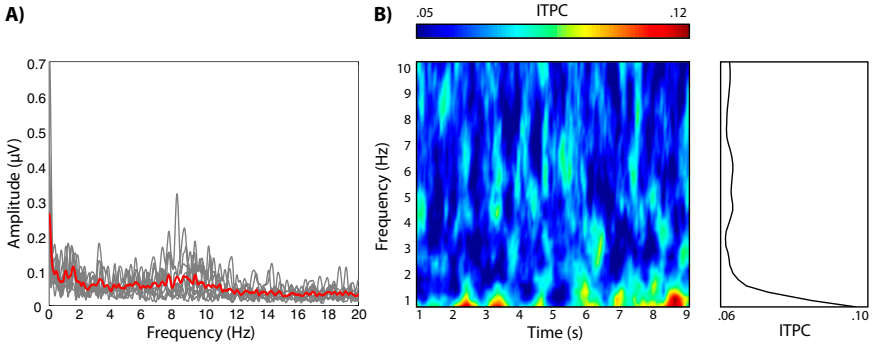

Fig. S1. No evidence for entrainment was observed when amplitude spectra and ITPC were calculated for trials that were not realigned to a common stimulus phase. (*A*) Amplitude spectrum of FFT of time-domain EEG signal. Red line indicates the group average spectrum, and gray lines show single participants' spectra, averaged over all electrodes. Individual trials were time locked to the stimulus onset and were not realigned with respect to per-trial stimulus phase. Amplitude in the 3-Hz and 6-Hz frequency bins did not differ significantly from amplitude in the neighboring bins [3 Hz: $t_{(11)}= -1.91$, $P = 0.08$; 6 Hz: $t_{(11)} = -1.71$, $P = 0.12$], and the trend was in the wrong direction. (*B*) ITPC shown over time (*Left*) and averaged over time (*Right*), again averaged over all electrodes. A permutation *t* test on ITPC (Fig. S2*B*) failed to reveal any frequency bands in which ITPC was significantly higher than during the prestimulus baseline period.

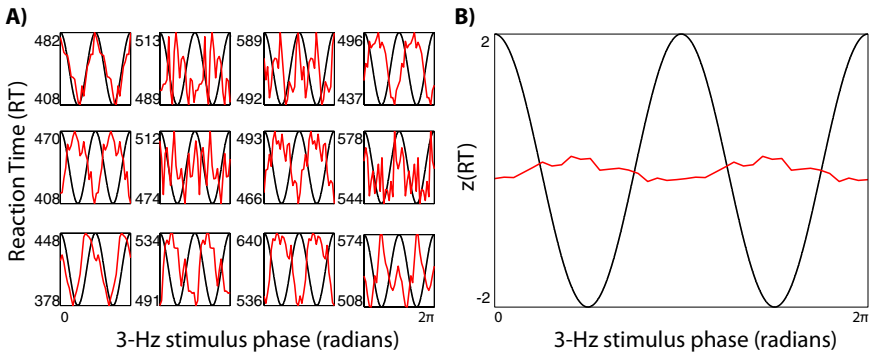

Fig. S2. (*A*) RTs to detected gaps were modulated by stimulus phase. Squared, arcsine-transformed, circular-linear correlation coefficients were calculated for each individual and tested against the null hypothesis of zero correlation. RTs were significantly correlated with stimulus phase [rms $\rho = 0.70$, $t_{(11)} = 6.74$, $P < 0.001$]. (*B*) However, grand average RTs (z-transformed before averaging) were not systematically related to stimulus phase, ruling out an acoustic explanation for the behavioral modulation.

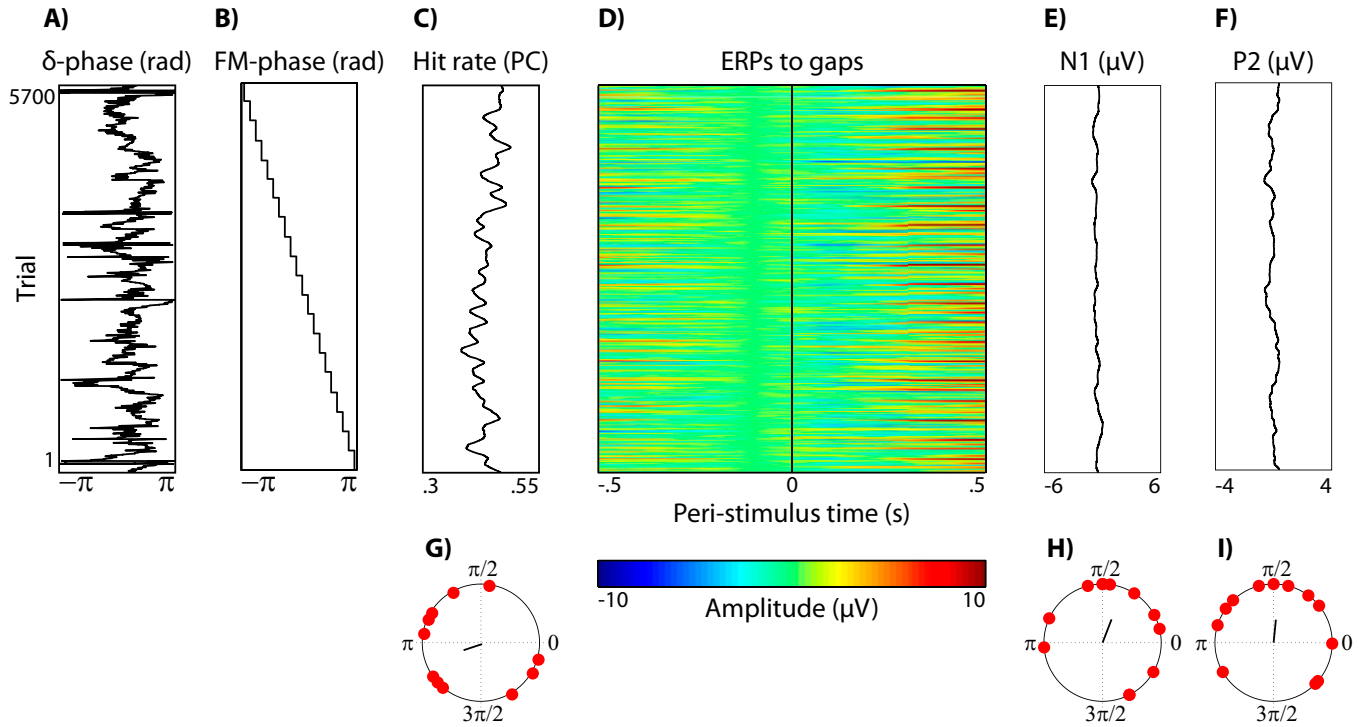

Fig. S3. No systematic relation between stimulus phase and hit rate or ERPs was observed across listeners. Trials were sorted according to single-trial stimulus phase (*B*) rather than single-trial delta brain phase (*A*). Neither hit rate (*C*) nor ERPs (*D*–*F*) were systematically related to stimulus phase across listeners. Hit rates (*C*), N1 amplitude (*E*), and P2 amplitude (*F*) were each significantly correlated with stimulus phase within listeners. However, optimal stimulus phase defined in terms of hit rate (*G*), N1 amplitude (*H*), and P2 amplitude (*I*) was not consistent across listeners (Rayleigh's tests, all $P \geq 0.16$).

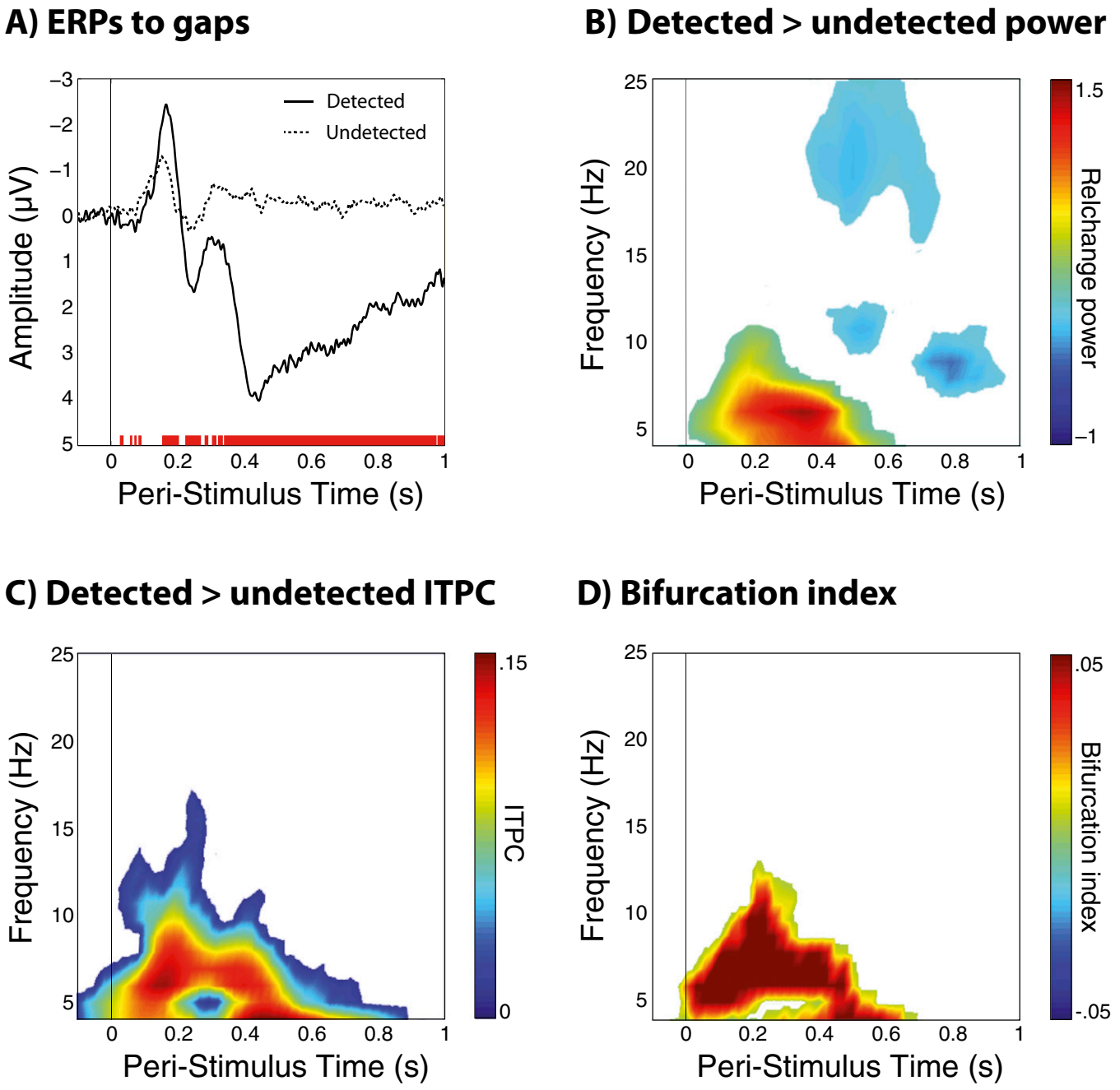

Fig. S4. Comparison of detected and undetected gaps. (*A*) ERPs to detected gaps were larger than to undetected gaps; red bar marks areas of significant difference. (*B*) Significant cluster for total power: detected > undetected gaps. A delta-theta-alpha enhancement during the time window of the ERP was larger for detected gaps, as were later suppressions in the alpha and beta ranges. (*C*) Significant cluster for ITPC for the contrast detected > undetected gaps. One significant cluster in the delta-theta-alpha range during the time window of the ERP revealed increased phase locking for detected relative to undetected gaps. (*D*) Significant cluster for the bifurcation index. One significant cluster in the delta-theta-alpha range during the time window of the ERP revealed that detected gaps reset the phase in the 2- to 12-Hz band more consistently than undetected gaps.

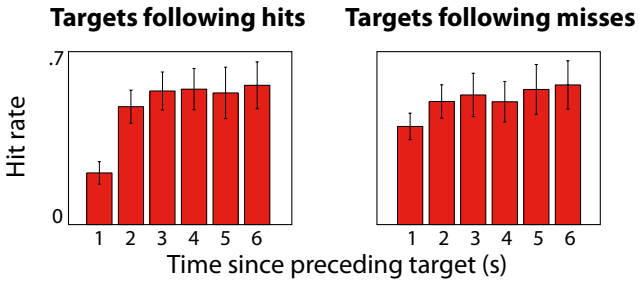

Fig. S5. Hit rates plotted as a function of the time since the previous gap, separately for cases when the previous gap was a hit (*Left*) versus when it was a miss (*Right*). Hit rates were significantly reduced for targets after a hit within 1 s relative to targets after a miss within 1 s.